

*Full Length Research Paper*

# Sensing and filtering characteristics of electrostatic sensors for pneumatically conveyed particles

M. F. Rahmat<sup>1</sup>, I. T. Thuku<sup>1</sup>, T. Tajdari<sup>1</sup>, K. Jusoff<sup>2\*</sup> and M. R. Ghazali<sup>3</sup>

<sup>1</sup>Department of Control and Instrumentation Engineering, Faculty of Electrical Engineering, Universiti Teknologi Malaysia, 81310 Skudai Johor, Malaysia.

<sup>2</sup>Faculty of Forestry, Universiti Putra Malaysia, 43400 Serdang, Selangor, Malaysia.

<sup>3</sup>Faculty of Electrical and Electronic Engineering, Universiti Malaysia Pahang, Kampus Pekan, 26600 Pekan Pahang, Malaysia.

Accepted 20 July 2011

**Electrostatic sensor, which can also be called as triboelectric sensor or electrodynamic sensor, senses the electrostatic charge carried by the dry particle in pneumatic conveyor. Source of the signal induced on the electrostatic sensor is brought by the object to be measured and no excitation circuit is necessary. Electrostatic sensors are used in the process industry due their low cost and robust. This paper describes an investigation into characteristics of circular and rectangular plate shapes of electrostatic sensors. Two parameters were investigated, the effect of sensor area on sensitivity and the spatial filtering effect of the sensor due to its finite size. Models were proposed and results obtained and used to compare with experimental values. It was observed that relationships existed between sensor sensitivity, sensor area and sensor spatial filtering effect.**

**Key words:** Electrostatic sensor, sensitivity, spatial filtering, electrodynamic sensor.

## INTRODUCTION

Movement of particle in pipeline generates an electrostatic charge. Electrostatic charge can be detected using sensing device or electrode. This electrostatic charge is converted into voltage by associated electronic or electrodynamic transducer. Transducers which sense the electrostatic charge carried by dry solids have applications in determining flow parameters in pneumatic conveyors for example, the velocity of conveyed materials (Featherstone et al., 1983; Wen et al., 2011) and the solids volume flow rate (Gajewski, 1999). The measurement is based on charge being induced into the sensor as the charged particles flow past it. Sensors generally consist of areas of metal insulated from the walls of the conveyor. For process measurement ring electrodes are widely used and have been thoroughly investigated (Ma et al., 2000; Yan et al., 1995; Zhang and Yan, 2003).

Electrostatic sensors are robust and low cost, thus have the potential to be applied for process tomography.

In process tomography (William and Beck, 1995) several identical sensors are positioned around the vessel being interrogated to provide measurements which are used to reconstruct dynamic images of the movement of the material being monitored. With large numbers of sensors (Abdalla et al., 2011) the ring electrode is no longer applicable and small sensors (Nejati and Khoshbin, 2010) consisting of either rectangular or circular plate section are more appropriate.

For circular plate shape as shown in Figure 1, with a particle p, carrying a charge q, traveling at a uniform velocity V, constrained to pass a conducting circular electrode is shown in below along a path which is perpendicular to the vertical axis of the electrode Figure 2.

The electric field, E, due to charged particle at a distance PQ is:

$$E = \frac{q}{4\pi\epsilon_0(PQ)^2} \quad (1)$$

\*Corresponding author. E-mail: [kjusoff@yahoo.com](mailto:kjusoff@yahoo.com)

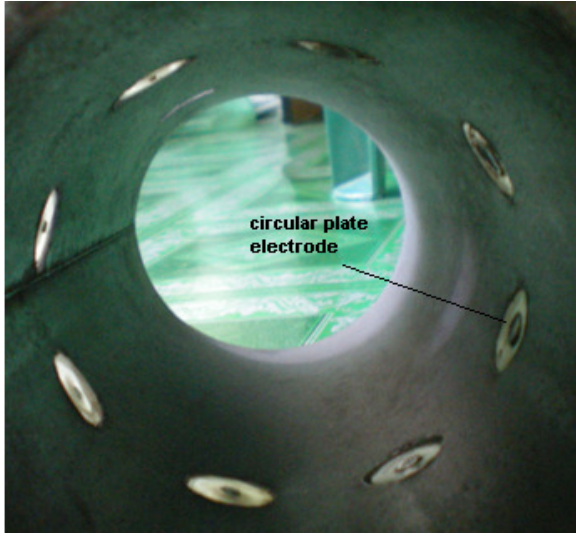


Figure 1. 5 mm circular plate electrode mounted in the pipe.

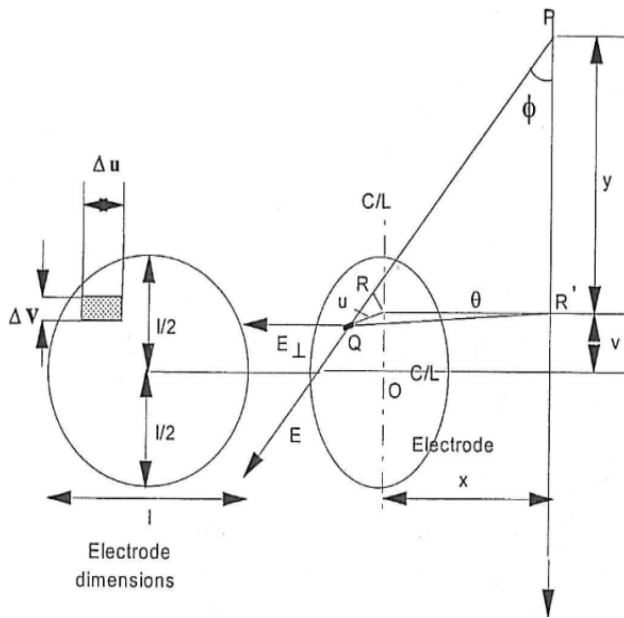


Figure 2. Isometric view of a charged particle approaching a flat ended circular plate electrode.

The component of this field normal to the sensor at this point,  $E_{\perp}$ , is

$$E_{\perp} = E \sin \phi \cos \theta \quad (2)$$

where  $\sin \phi = \frac{QR'}{QP}$  and  $\cos \theta = \frac{x}{QR'}$ .

$$E_{\perp} = E \cdot \frac{QR'}{QP} \cdot \frac{x}{QR'} \quad (3)$$

$$E_{\perp} = E \cdot \frac{x}{QP}$$

Substituting from Equation (1) into (3) yields Equation (4),

$$E_{\perp} = \frac{q}{4\pi\epsilon_0 (QP)^2} \cdot \frac{x}{QP} \quad (4)$$

From Figure 2,

$$(QP)^2 = (y-v)^2 + (QR')^2 \quad (5)$$

where  $(QR')^2 = u^2 + x^2$  then Equation (4) is given by;

$$E_{\perp} = \frac{qx}{4\pi\epsilon_0 \left\{ (y-v)^2 + u^2 + x^2 \right\}^{\frac{3}{2}}} \quad (6)$$

The charge induced into a small element of electrode of area  $\delta_s$  is,

$$dq' = -\epsilon_0 E_{\perp} \delta_s \quad (7)$$

Substituting for  $E_{\perp}$  and  $\delta_s = \Delta u \cdot \Delta v$ .

$$dq' = -\epsilon_0 \frac{qx}{4\pi\epsilon_0 \left\{ (y-v)^2 + u^2 + x^2 \right\}^{\frac{3}{2}}} \cdot \Delta u \cdot \Delta v \quad (8)$$

Equation (8) must be integrated over the whole circular cross section of the section of the sensor to determine the induced charge total as shown in Equation (9).

$$q' = -\frac{qx}{2\pi} \int_{-\frac{l}{2}}^{\frac{l}{2}} dv \cdot \int_{u=0}^{\sqrt{\frac{l^2}{4}-v^2}} \frac{du}{\left\{ (y-v)^2 + u^2 + x^2 \right\}^{\frac{3}{2}}} \quad (9)$$

$$q' = -\frac{qx}{2\pi} \int_{-\frac{l}{2}}^{\frac{l}{2}} \frac{\sqrt{l^2-4v^2} dv}{\left( x^2 + (y-v)^2 \right) \cdot (4x^2 + 4y^2 - 8yv + l^2)} \quad (10)$$



**Figure 3.** Rectangular plate electrodes mounted inside the pipe.

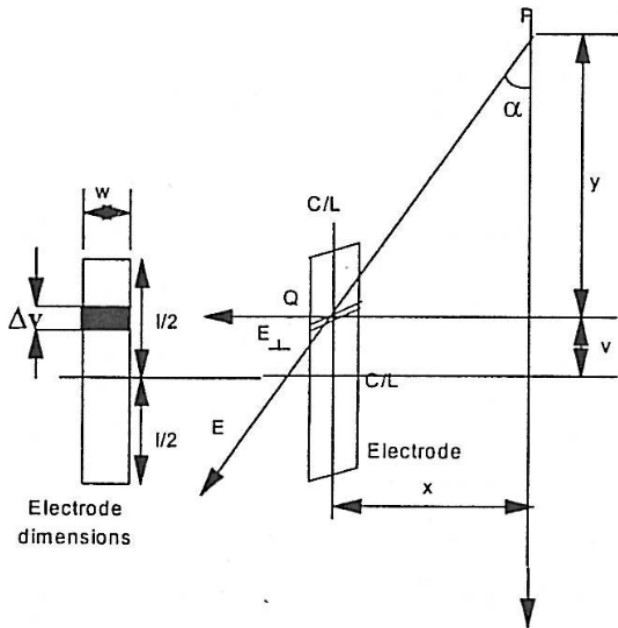


**Figure 4.** Isometric view of a charged particle approaching a rectangular plate electrode.

Equation (10) cannot be solved implicitly. From Equation (10), the current,  $i'$  is given by;

$$i' = \frac{dq'}{dt} \text{ where } y = Vt .$$

In rectangular shape plate electrode, Figure 3, particle p which carries a charge q, traveling at a uniform velocity V, constrained to pass a conducting rectangular electrode

as shown in Figure 4. The electric field, E, due to charged particle at a distance PQ is;

$$E = \frac{q}{4\pi\epsilon_0(PQ)^2} \tag{11}$$

The component of this field normal to the sensor at this point,  $E_{\perp}$ , is;

$$E = \frac{q}{4\pi\epsilon_0(PQ)^2} \sin \alpha \tag{12}$$

The charge induced into a small element of electrode of area  $\delta_s$  is,

$$dq' = -\epsilon_0 E_{\perp} \delta_s \tag{13}$$

Substituting for  $E_{\perp}$  and  $\delta_s = w\Delta v$  in to (13), then;

$$dq' = -\epsilon_0 \frac{q}{4\pi\epsilon_0(PQ)^2} \sin \alpha w\Delta v \tag{14}$$

With  $\sin \alpha = \frac{x}{(PQ)}$  then;

$$dq' = -\frac{qx}{4\pi} \cdot \frac{w}{(PQ)^3} \cdot \Delta v \tag{15}$$

From Figure 4,  $(PQ)^2 = (y-v)^2 + x^2$

Therefore the charge induced into the element  $\delta_s$  is,

$$dq' = -\frac{qxw}{4\pi} \cdot \frac{\Delta v}{\{(y-v)^2 + x^2\}^{\frac{3}{2}}} \tag{16}$$

Therefore the total charge induced into the sensor is given by;

$$q' = -\frac{qxw}{4\pi} \cdot \int_{-\frac{l}{2}}^{\frac{l}{2}} \frac{dv}{\{(y-v)^2 + x^2\}^{\frac{3}{2}}} \tag{17}$$

This has been integrated using derive software giving,

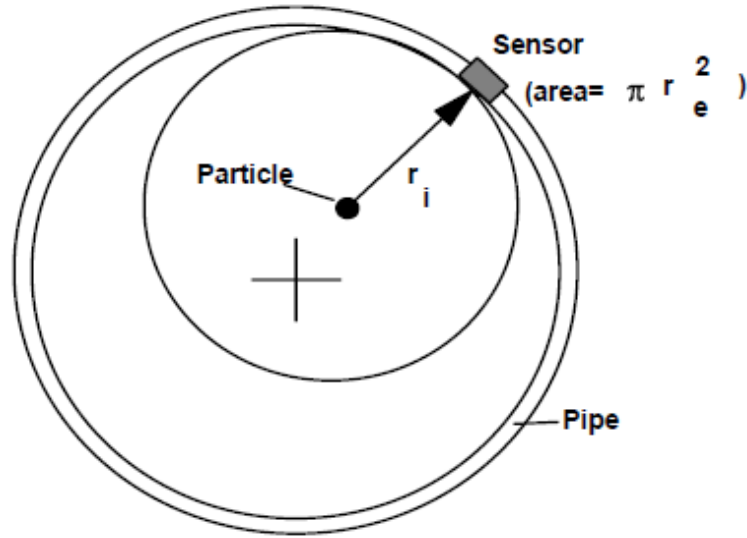


Figure 5. Positional relationship between particle and sensor.

$$q' = -\frac{qxw}{4\pi} \left[ \frac{1}{x^2} \left\{ \frac{\left(y + \frac{l}{2}\right)}{\left[y^2 + yl + \frac{l^2}{2} + x^2\right]^2} - \frac{\left(y - \frac{l}{2}\right)}{\left[y^2 - yl + \frac{l^2}{2} + x^2\right]^2} \right\} \right] \quad (18)$$

From Equation (18), the current,  $i'$  is given by  $i' = \frac{dq'}{dt}$ , where  $y = Vt$ .

For applications where the process is varying rapidly, for example pneumatically conveyed solids, the measurement system parameters should be known. This paper investigates the relationships between sensor size, sensor sensitivity and the frequency bandwidth, termed the spatial filtering effect of the transduced signals where ring and rectangular electrodes spatial sensitivity and spatial filtering effect are well investigated in Krabicka and Yan (2009), Peng et al. (2008), and Xu et al. (2009, 2007).

**METHODOLOGY**

**Electrode sensitivity**

The electrode sensitivity is modeled for a circular electrode by considering the effect of a single charged particle,  $q$ , as it moves vertically downwards at a constant velocity,  $v$ . The assumptions for the model are, the point charge is travelling in an axial direction parallel to the axis of the pipe, the particle has a constant finite amount of charge which is not dissipated during the time it travels through the sensing volume, the surface area of the electrode is small compared to the radius of the pipe and the charge acts as a point source and the pipe is of non conducting material. Then for a

single charged particle, assumed to be a point charge of value  $q$ , the field is uniformly radial.

$$E = \frac{q}{4\pi r_i^2 \epsilon_0} \quad (19)$$

This point charge induces a potential onto the surface of the small, flat electrode used to sense the change in potential at a point on the wall of a non-conducting or dielectric pipe. It is assumed that there are no other interacting fields on the electrode since there is no surface charge on the pipe wall. For a given circular sensor, the surface area is  $\pi r_e^2$  which is considered normal to the flux as shown in Figure 5. So the proportion of flux passing through the sensor due to the charged particle at a distance  $r_i$  is,

$$\frac{\pi r_e^2}{4\pi r_i^2} \quad (20)$$

The charge induced onto the sensor is proportional to  $q$ . Hence,

$$Q_e = \frac{kq r_e^2}{r_i^2} \quad (21)$$

Equation 21 suggests that the amount of charge induced onto an electrode depends upon the radius of the electrode squared, that is, the area of the electrode. This charge is stored on a capacitor and provides a voltage  $V_e$  given by;

$$Q_e = CV_e \quad (22)$$

The voltage is amplified, rectified, smoothed and averaged. The sensitivity of the sensor is defined as  $Q_e / q_i$ . This value is difficult

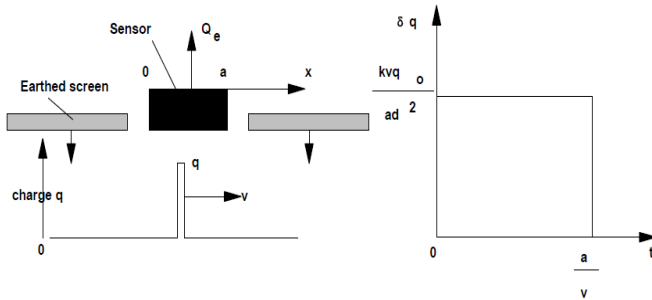


Figure 6. The measurement parameters.

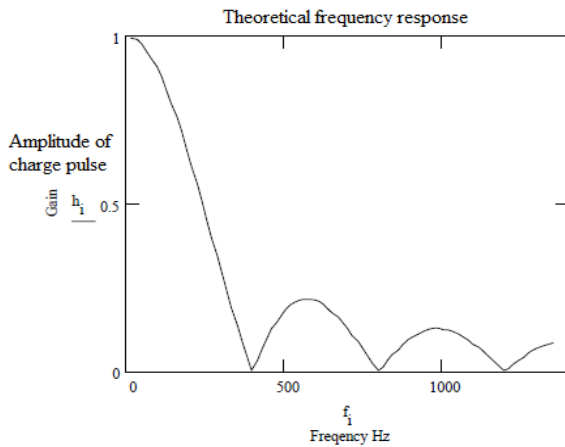


Figure 7. Frequency response for a = 0.005 mm, v = 2.0 m/s

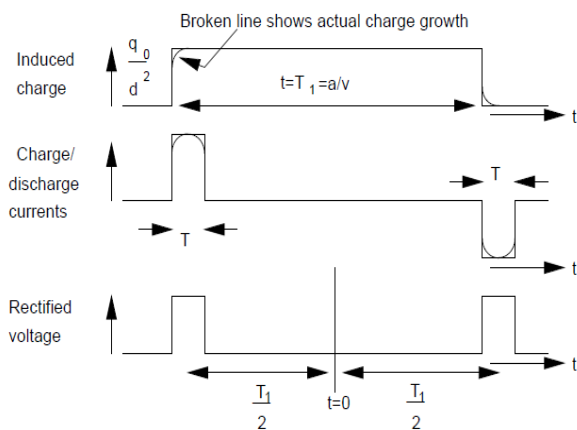


Figure 8. Idealised induced charge and corresponding voltages for the rectangular electrode.

to determine because the level of the conveyed charge,  $q_i$ , is difficult to control. In this paper, the same particles, and hence charges, pass a series of sensors of different diameters in order

to compare sensitivity.

**Spatial filtering effect**

An investigation into the spatial filtering effect arising from capacitance electrodes is described in a paper by Hammer and Green (1983), which relates the velocity of flowing discontinuous material to the frequency bandwidth of the sensed signal (Gajewski, 1996, 2000). This paper extends the concept to electrodynamic sensors. Process tomography using electrodynamic sensors will generally use circular or rectangular electrodes, however, there may be applications requiring rectangular electrodes (Machida and Scarlett, 2005). The results from the rectangular electrodes may be compared with the measurements obtained using capacitance electrodes (Hammer and Green, 1983).

For circular electrode assume that a single charged particle moves past the sensor, of diameter or length  $a$ , at a distance  $d$ , with a velocity  $v$ , can be considered as a pulse of charge  $q(t)$ . This moving charge results in a charge being induced into the sensor as shown in Figure 4. The quantity of charge induced into the sensor is described by;

$$\delta q_i = k \frac{v}{a} \int_0^\infty \frac{q(t)}{d^2} dt \tag{23}$$

where  $q(t)$  represents the charge pulse provided by the moving particle and  $k$  is a constant of proportionality with appropriate dimensions. If the pulse duration is short compared with  $a/v$  it may be shown (Hammer and Green, 1983) that the response is a 'sinc' function with the effect of  $a$  and  $v$  on the modulus as shown graphically in Figure 6.

The amplitude frequency response for Equation (23) after derivation as discussed in Rahmat et al. (2009, 2009) may be written as follows.

$$|h(j\omega)| = k \left| \frac{\sin\left(\frac{\omega a}{2v}\right)}{\frac{\omega a}{2v}} \right| \tag{24}$$

This transfer function is plotted as shown in Figure 7.

Transfer function minimum occur when  $\sin\left(\frac{\omega a}{2v}\right) = 0$ , therefore

$$\frac{\omega a}{2v} = \pi, 2\pi, 3\pi \text{ and minimum when } \frac{v}{a} = \frac{\omega}{2\pi}, \frac{\omega}{4\pi}, \frac{\omega}{6\pi} \dots$$

The rectangular electrode are much longer than the circular electrode ones and recordings of the voltage from the sensor, taken when investigating the spatial filtering effect, are slightly different from those from the flat ended, circular electrodes. The analysis of curve requires modification to determine the spatial filtering characteristic of long rectangular sensors.

In the experimental verification of this analysis, the long electrodes are curved to approximately the same radius as the charged bead moves along to ensure the bead electrode gap remains constant as it passes. In this case the charged bead is passing the electrode for a longer period than for the circular sensor. The charge and discharge currents are noticeably spaced in time, as are the corresponding rectified voltages as shown in Figure 8.

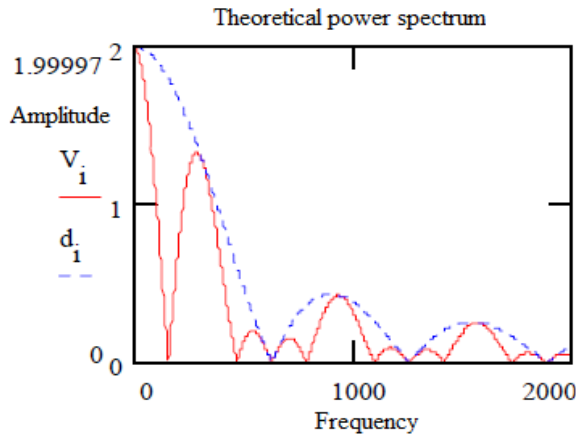


Figure 9. Predicted spatial frequency response for the rectangular electrode.

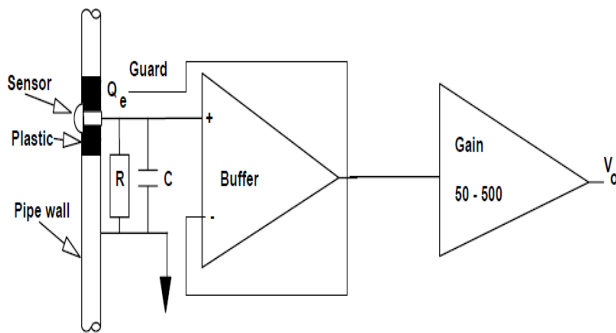


Figure 10. The electrostatic sensor circuit.

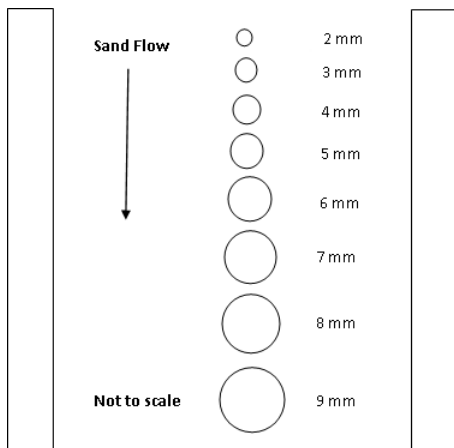


Figure 11. Arrangement of circular electrodes for sensitivity measurements.

The spatial filtering effect for this system is calculated by considering the system as consisting of two impulses with a time delay separating them. If the pulse duration's are short compared with  $a/v$  they may be regarded as two Dirac pulses.

Then the transducer response may be written as;

$$v_i(\omega) = \int_{-\frac{T_1+T}{2}}^{\frac{T_1+T}{2}} k \frac{q_0}{d^2} e^{j\omega t} dt + \int_{\frac{T_1-T}{2}}^{\frac{T_1+T}{2}} k \frac{q_0}{d^2} e^{j\omega t} dt \quad (25)$$

where T is the time taken to charge and discharge the electrode. After integration and expansion, Equation (25) gives;

$$\frac{V_i}{q_0} = \frac{4k}{d^2 \omega} \cos \frac{\omega T_1}{2} \sin \frac{\omega T}{2} \quad (26)$$

This may be written in the frequency domain. The modulus of Equation (26) is given by,

$$\left| \frac{V_i}{q_0} \right| = \frac{2k}{d^2} \left| \cos \frac{\omega a}{2v} \right| \left| \frac{\sin \left( \frac{\omega T}{2} \right)}{\frac{\omega}{2}} \right| \quad (27)$$

and the effect of 'a' and 'v' on the modulus shown the sinc and cos function which is graphically shown in Figure 9.

**Electrodynamic sensor**

The circuit diagram of the electrostatic sensor is shown in Figure 10, the sensor consists of a plain metal rod, termed the electrode, which is isolated from the walls of the metal conveying pipe by an insulator, for example glass or plastic. This electrode has a capacitance to earth, which is very small (fraction of a pico Farad) but variable due to manufacturing tolerances. To minimise the effect of this capacitance a low value capacitor (several pico Farad) is connected in parallel with it. A resistor is connected in parallel with the capacitors to provide a charge/discharge path. The charged particles in the pipe flow past the electrode inducing charge into it in the process. The flow of current through the resistor due to this induced charge results in a varying voltage. This voltage is buffered by a unity gain non inverting amplifier whose output provides a driven guard for the input circuitry and is amplified and conditioned by further circuitry.

**RESULTS AND DISCUSSION**

Results from two experiments are presented. The first experiment is used to determine the sensitivity of circular and rectangular electrode in several of size areas. The second experiment investigates the spatial filtering effect of the electrode in several size electrodes.

**Sensor sensitivity**

The sensitivity is determined by arranging a number of differently sized sensors so that sand flows past each of them as shown in Figure 11.

The sensor are installed close to each other, in a way that the distance from top sensor to bottom sensor is not

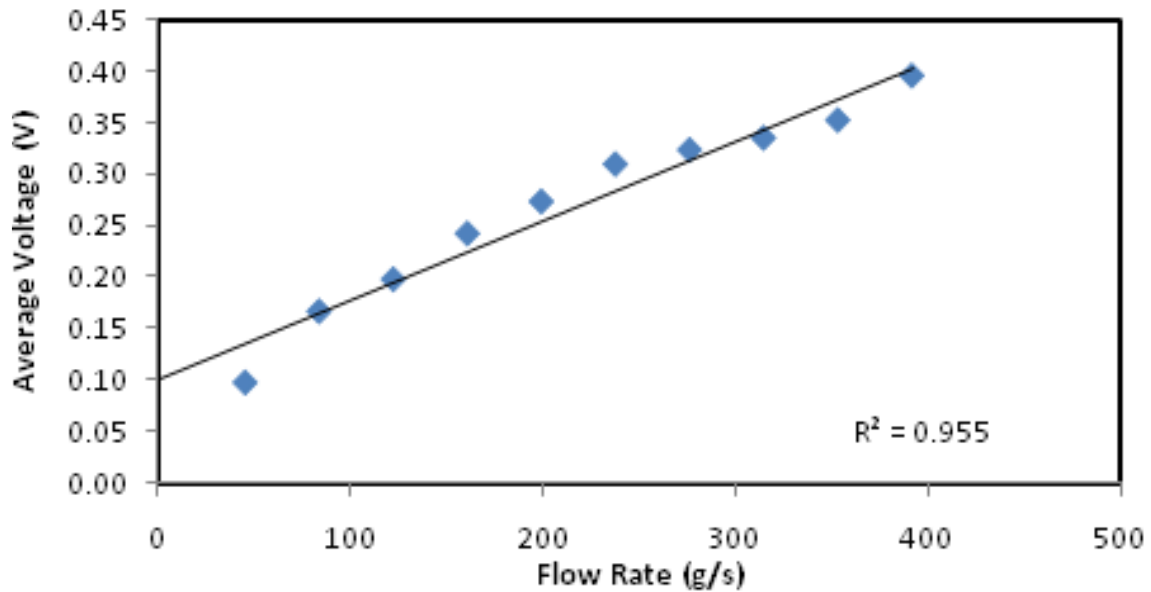


Figure 12. Sensitivity for 4 mm circular electrode.

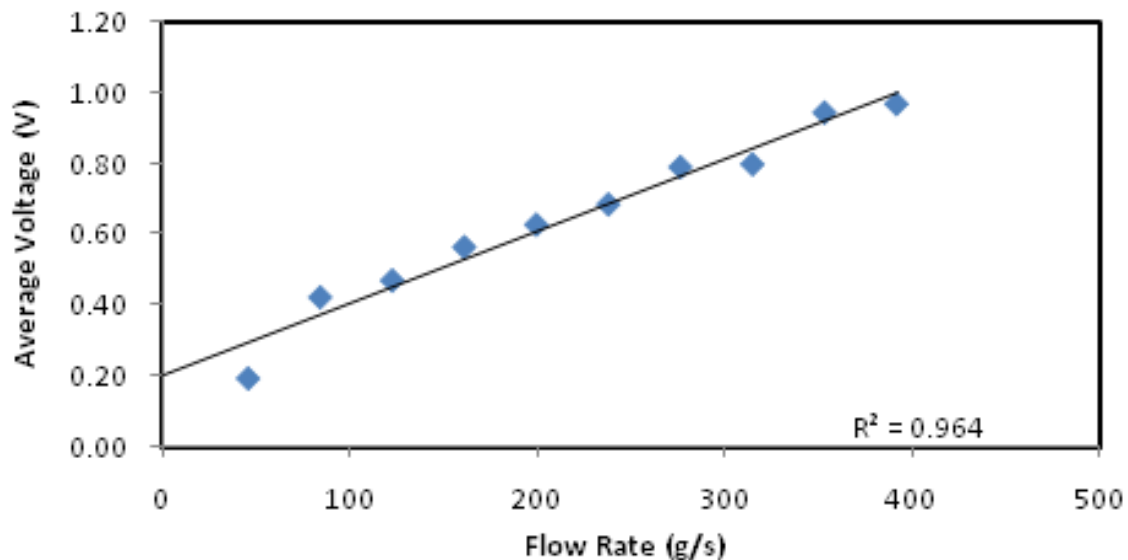


Figure 13. Sensitivity for 7 mm circular electrode.

more than 20 cm, so the small change in electrical charge of the bead due to traversing this distance assume to be zero and sensors are sensing the same electrical charge. The level of charge on the flowing sand is very difficult to quantify, however since the sensors are evaluated at the same time their outputs may be compared directly. The small diameter electrode at each end of the array checks that the flowing sand does not change its characteristics as it traverses the section.

A series of different sand flow rates are made to pass the electrodes and the resulting outputs determined. The tests were conducted for the electrode with size from 2 to 9 mm diameter. The results for the sensor sensitivity of 4, 7 and 9 mm diameter electrode are shown in Figures 12 to 14.

A linear regression line is fitted to the measured values. The gradient of this line provides the overall sensitivity of the sensor (mV/g/s) and summarized in

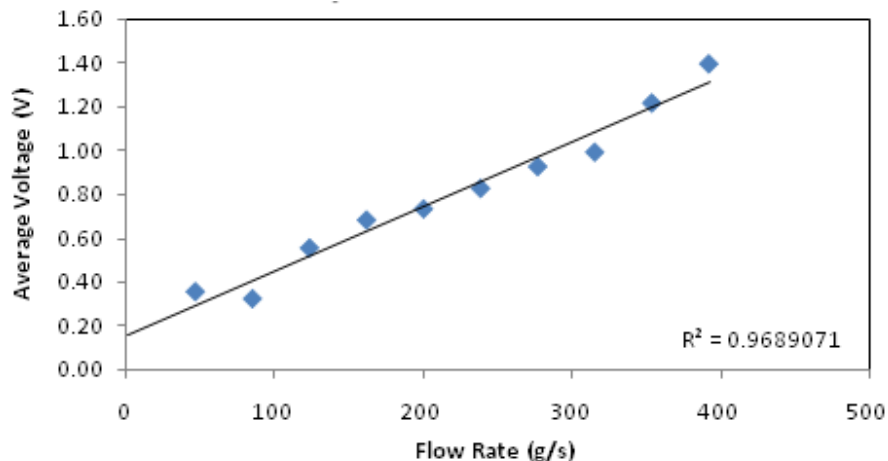


Figure 14. Sensitivity for 9 mm circular electrode.

Table 1. Electrode sensitivity of electrostatic sensor.

Electrode diameter (mm)	Electrode area (mm) <sup>2</sup>	Transducer sensitivity (mV/g/s)	Electronic gain	Electrode sensitivity (mV/g/s)
2	3.14	0.631	150	$4.21 \times 10^{-3}$
3	7.07	0.504	150	$3.36 \times 10^{-3}$
4	12.57	0.775	150	$5.17 \times 10^{-3}$
5	19.64	1.384	150	$9.22 \times 10^{-3}$
6	28.28	1.512	150	$1.01 \times 10^{-2}$
7	38.49	2.050	150	$1.37 \times 10^{-2}$
8	50.27	3.395	150	$2.26 \times 10^{-2}$
9	63.62	2.149	150	$1.96 \times 10^{-2}$

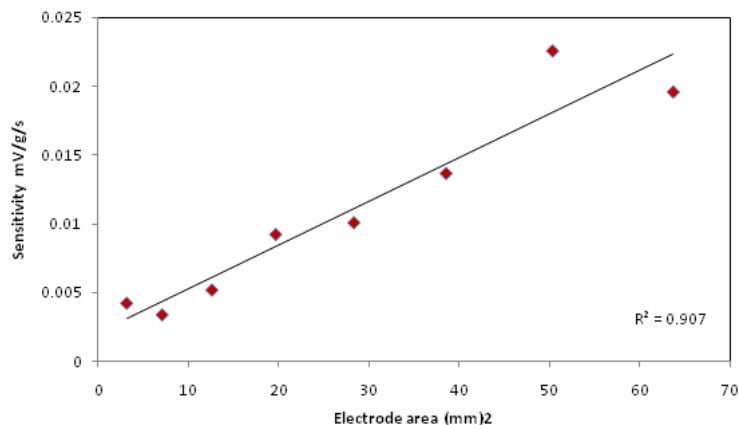
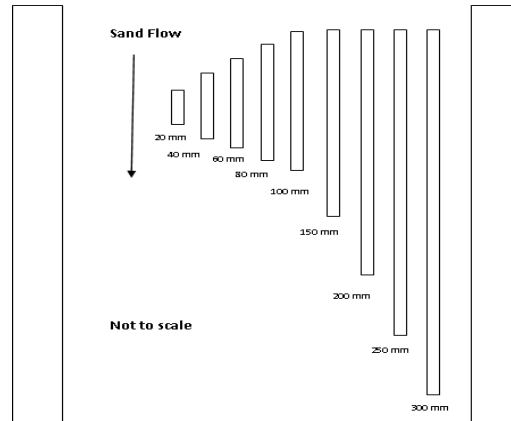


Figure 15. Plot showing sensitivity versus electrode area for circular sensor.

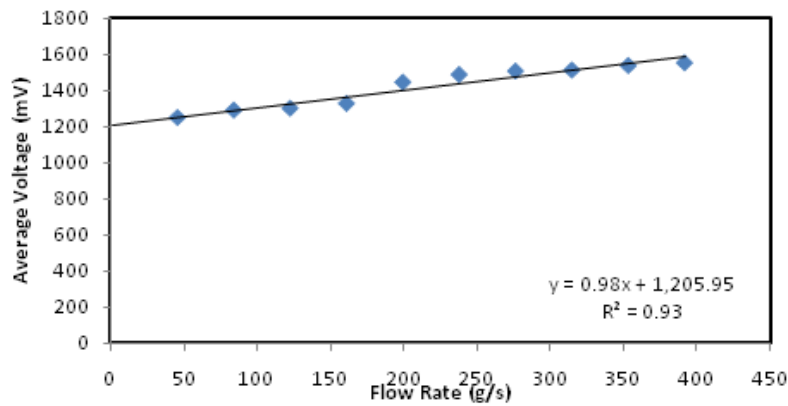
Table 1 and Figure 15. In order to observe the relationship of sensor sensitivity and sizes electrode, the transducer sensitivity of each size electrodes need to be divided by the gain of 150.

Table 1 shows the calculation of electrode sensitivity

and the results are shown in Figure 15. The result shows that the linear relation between electrode sensitivity and area of circular electrodes. Increasing of diameter or size of electrode will increase the sensitivity of sensor. Diameter 2 and 3 mm show the best fit or coefficient line



**Figure 16.** Arrangement of rectangular electrodes for sensitivity measurements.



**Figure 17.** Sensitivity for 20 mm length rectangular electrode.

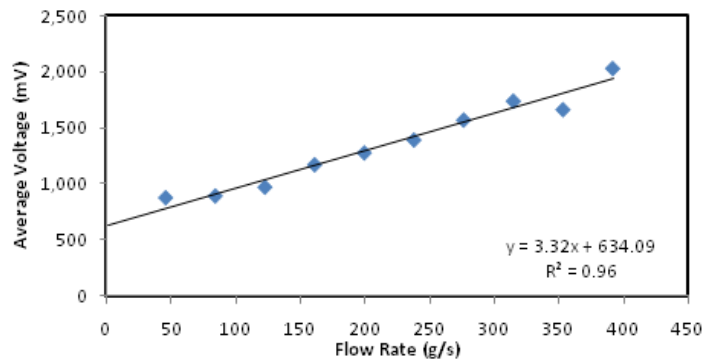


**Figure 18.** Sensitivity for 100 mm length rectangular electrode.

less than 90% and show that the measurement of small diameter is not stable for circular electrode.

The tests were repeated using rectangular electrodes 10 mm wide, but with lengths ranging from 20 to 300 mm. Similar analyses were carried out on the results. Figure

16 shows the arrangement of nine rectangular electrode for the width is fix to 10 mm and the length is 20, 40, 60, 80, 100, 150, 200, 250 and 300 mm.

Figures 17 to 19 show the sample of the results for sensor sensitivity versus flow rate for the rectangular

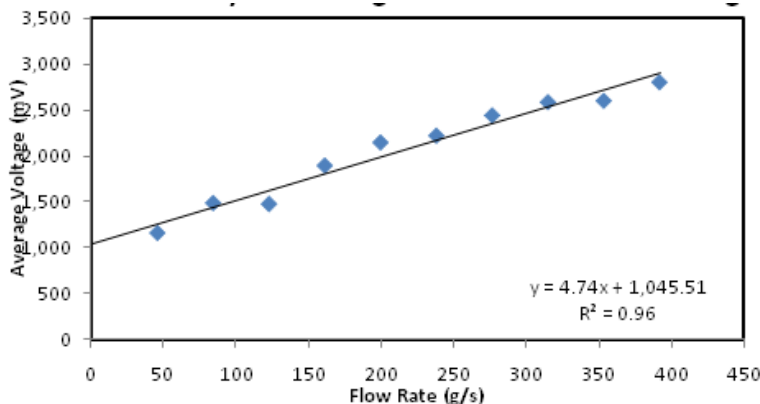


Figure 19. Sensitivity for 300 mm length rectangular electrode.

Table 2. Electrode sensitivity of rectangular electrode.

Electrode length (mm)	Area electrode (mm) <sup>2</sup>	Transducer sensitivity (mV/g/s)	Electronic gain	Electrode sensitivity (mV/g/s)
20	200	0.98	150	0.0065
40	400	1.65	150	0.0110
60	600	1.74	150	0.0116
80	800	2.33	150	0.0155
100	1000	3.32	150	0.0221
150	1500	3.96	150	0.0264
200	2000	4.44	150	0.0296
250	2500	4.61	150	0.0307

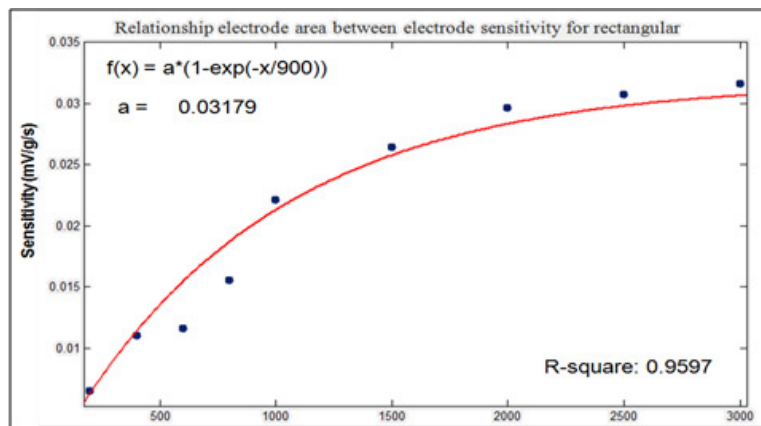


Figure 20. Plot showing sensitivity versus area of electrode (rectangular sensors).

electrodes that is, 20, 100 and 300 mm length.

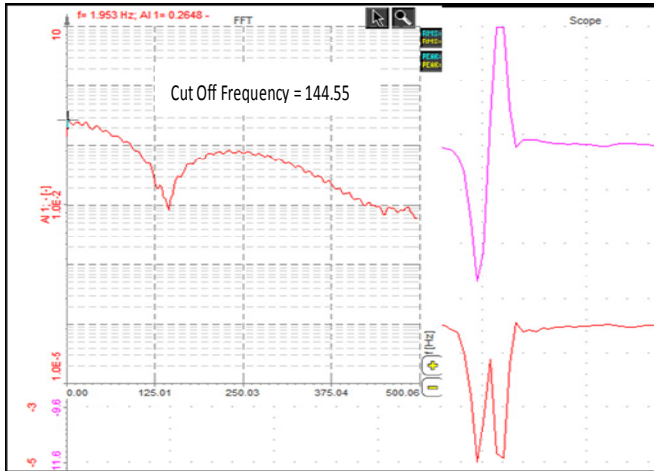
Analyses were carried out on the results and all the test are summarised in Table 2 and graphically shown in Figure 20.

Figure 20 shows that the non-linear relation between electrode sensitivity and area of rectangular electrodes. The best fit or coefficient line is 95.97% and the result

shows for the long length of rectangular electrode, sensitivity is asymptotically increases to 0.03179 mV/g/s.

#### **Spatial filtering effect**

For spatial filtering effect analysis, rectified voltage signal



**Figure 21.** Rectified voltages on time and frequency domain for diameter 2 mm, which occurred at cut off frequency at 144.55 Hz.

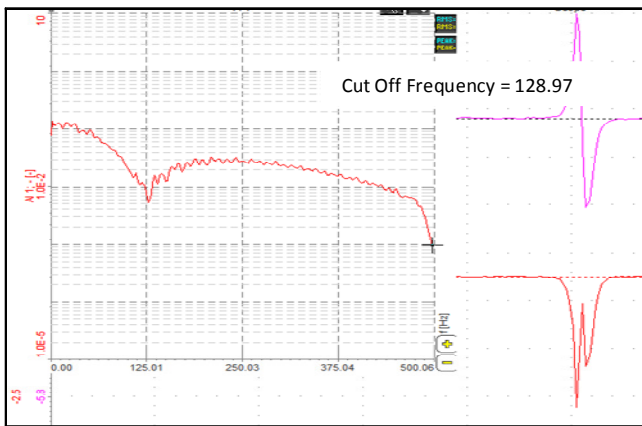


**Figure 22.** Rectified voltage on time and frequency domain for diameter 5 mm, which occurred at cut off frequency of 128.97 Hz.

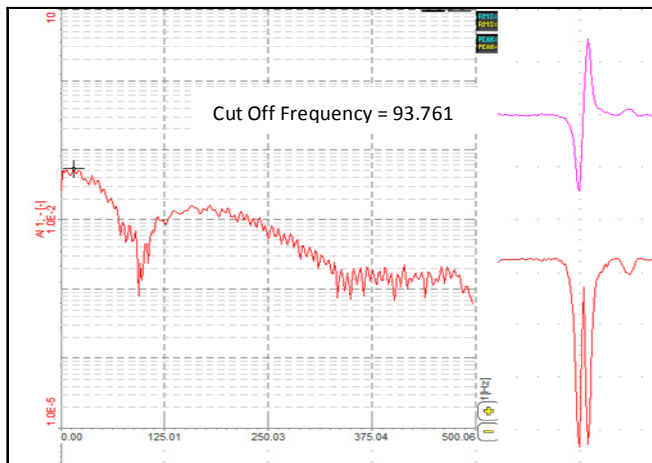


**Figure 23.** Rectified voltage on time and frequency domain for diameter 9 mm, which occurred at cut off frequency of 93.76 Hz.

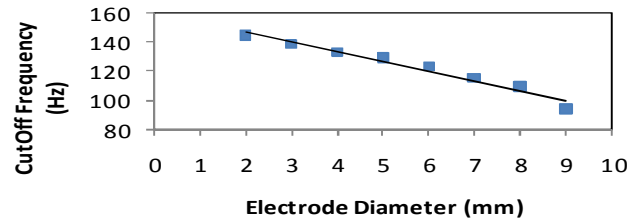


**Figure 24.** Relation between cut off frequency with diameter for circular electrodes.

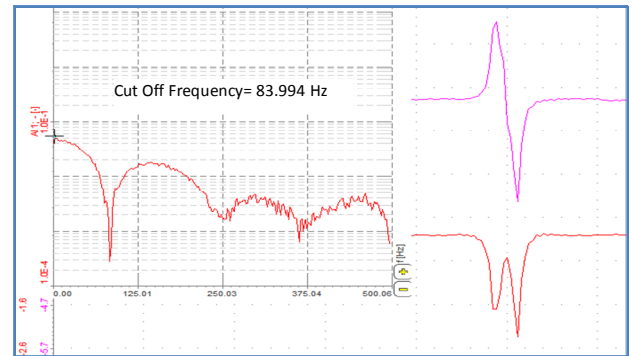


**Figure 25.** Rectified voltage on time and frequency domain for length of 20 mm, which occurred cut off frequency at 83.99 Hz.

measured by electrodynamic transducer will be inverted and converted into frequency domain using Fourier transform concept. The result for circular electrode on frequency spectrum is sinc function that follows the theory calculated as shown in Figure 7. This frequency spectrum can be observed in terms of cut off frequency obtained. The tests were conducted for the circular electrodes with diameter from 2 to 9 mm. The samples of the result of frequency spectrum for circular electrodes with diameter 2, 5 and 9 mm are shown in Figures 21 to 23 at mass flow rate, is 45.85 g/s.

On the right hand side of the figure show the signal in time domain which is non-inverting voltage and rectified voltage signal. The left hand side signal is frequency spectrum of rectified voltage. The result of frequency response obtained show that, all frequency spectrums are in same curve that are given in sinc function as shown in Equation (24). The characteristic of spatial filtering effect will continue with the relationship between cut off frequency and electrode length of electrodes and the result is shown in Figure 24.

From observation, increasing the diameter of circular electrode will decrease the cut off frequency in linear properties of gradient -6.674 Hz/mm.

The experiments were repeated using rectangular electrode with similar analyses were carried out for electrode length from 20 to 300 mm. Figures 25 to 27 show that the samples of the results obtained for

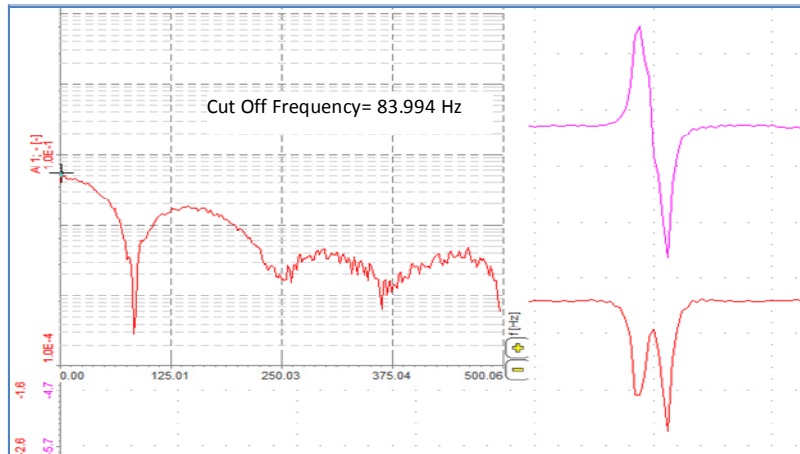


**Figure 26.** Rectified voltage on time and frequency domain for length of 100 mm, which occurred at cut off frequency of 43.3 Hz.



**Figure 27.** Rectified voltage on time and frequency domain for length of 300 mm, which occurred at cut off frequency of 29.55 Hz.

electrode length 20, 100 and 300 mm at mass flow rate is 45.89 g/s.

The right hand side of the figure shows the signal in time domain which is non-inverting voltage and rectified voltage signal. The left hand side of the figure shows the frequency spectrum of rectified voltage.

The result for rectangular electrode on frequency spectrum shows the combination of Sinc and Cos function that follows the theory calculated as in Equation (27) and Figure 9 respectively. This frequency spectrum can be observed in terms of cut off frequency acquired. The sensor characteristic of spatial filtering effect will continue with the relationship between cut off frequency and electrode area of rectangular electrodes and the result shown in Figure 28.

From observation, increasing the length of rectangular electrode will asymptotically decrease the cut off frequency to 30 Hz. The results shown in Figure 15 support the theory that the electrode sensitivity is a linear

function of electrode area for the circular sensors. However, Figure 20 demonstrates that for long electrodes, the sensitivity asymptotically increases to 0.03179 mV/g/s with an increasing length. The spatial filtering with circular electrodes produces two significant results. Firstly, the spatial filtering with circular electrodes shows that the cut off frequency will decrease linearly with increasing diameter shown in Figure 24 but rectangular electrodes demonstrates that for long electrodes, the cut off frequency asymptotically decreases to 30 Hz with increasing length shown in Figure 28.

## Conclusion

It can be concluded that linear relationship exist between circular size electrode and sensor sensitivity but a non linear relationship exist between rectangular size

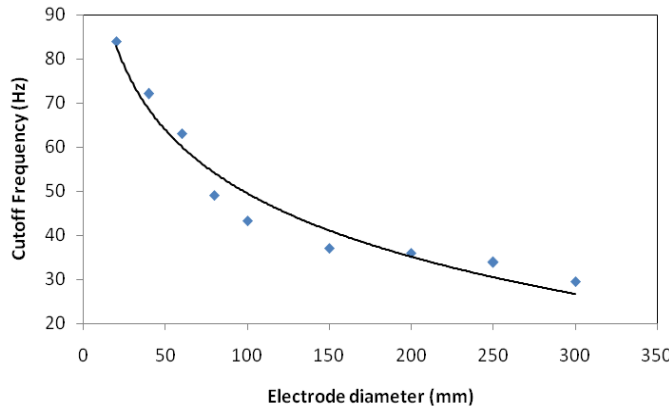


**Figure 28.** Relation of rectangular electrode on cut off frequency and electrode area.

electrode and sensor sensitivity. For spatial filtering effect investigation, the frequency response characteristics for a circular size electrode gave a sinc function response but for a rectangular size electrode gave a combination of sinc and cos function response. Both sensor sizes are suitable to be applied in process tomography and solid particle sizing investigation.

## ACKNOWLEDGEMENT

This research is supported by Ministry of Higher Education (MOHE) Malaysia and Universiti Teknologi Malaysia (UTM) through Research University Grant (GUP) Tier 1 vote number Q.J130000.7123.00H36. Authors are grateful to the Ministry and UTM for supporting the present work.

## REFERENCES

- Abdalla AN, Nubli M, Tan CS, Khairi F, Noraziah A (2011). Enhancement of real-time multi-patient monitoring system based on wireless sensor networks. *International J. Phys. Sci.* 6(4): 664-670.
- Featherstone AM, Green RG, Shackleton ME (1983). Yarn velocity measurement, *J Phys. E: Sci Instrum.* 16: 462-464.
- Gajewski JB (1996). Electrostatic inductive ring probe bandwidth. *Meas. Sci. Technol.* 7: 1766-1775.
- Gajewski JB (1999). Electrostatic flow probe and measuring system calibration for solids mass flow rate measurement. *J. Electrostat.* 45: 255-264.
- Gajewski JB (2000). Frequency response and bandwidth of an electrostatic flow probe. *J. Electron.* 48: 279-294.
- Hammer EA, Green RG (1983). The spatial filtering effect of capacitance transducer electrodes. *J. Phys. E: Sci. Instrum.* 16, 438-443.
- Krabicka J, Yan Y (2009). Finite-Element Modeling of Electrostatic Sensors for the Flow Measurement of Particles in Pneumatic Pipelines. *IEEE Transaction on Instrumentation and Measurement.* 58: 2730-2736.
- Ma J, Yan Y (2000). Design and evaluation of electrostatic sensors for the measurement of velocity of pneumatically conveyed solids. *Flow Measurement and Instrumentation.* 11:195-204.
- Machida M, Scarlett B (2005). Process tomography system by electrical charge carried by particle. *IEEE Sensors J.* 5: 252-259.
- Nejati F, Khoshbin H (2010). A novel secure and energy-efficient protocol for authentication in wireless sensor networks. *Int. J. Phys. Sci.* 5(10): 1558-1566.
- Peng L, Zhang Y, Yan Y (2008). Characterization of electrostatic sensors for flow measurement of particulate solids in square-shaped pneumatic conveying pipelines. *Sensors and Actuators.* 141: 59-67.
- Rahmat MF, Kamaruddin NS (2009). An electrodynamic sensor for electrostatic charge measurement. *Int. J. on Smart Sens. Intell. Syst.* 2: 200-212.
- Rahmat MF, Isa MD, Abdul Rahim R, Raja Hussin TA (2009). Electrodynamics sensor for image reconstruction process in an electrical charge tomography system. *Sensors.* 9: 10291-10308.
- Wen CC, Sheng CS, Kai HM (2011). An efficient inverter circuit design for driving the ultrasonic welding transducer. *Int. J. Phys. Sci.* 6(6): 1332-1341.
- William RA, Beck MS (1995). Principles, Techniques and Applications in Process Tomography, Butterworth-Heinemann Publisher. 1: 101-118.
- Xu Ch, Wang Sh, Tang G, Yang D, Zhou B (2007). Sensing characteristics of electrostatic inductive sensor for flow parameters measurement of pneumatically conveyed particles. *J. Electron.* 65: 282-592.
- Xu Ch, Tang G, Zhou B, Wang Sh (2009). The spatial filtering method for solid particle velocity measurement based on an electrostatic sensor. *Meas. Sci. Technol.* 20: 1-8.
- Yan Y, Byrne B, Woodhead S, Coulthard J (1995). Velocity measurement of pneumatically conveyed solids using electrodynamic sensors. *Meas. Sci. Technol.* 6: 515-537.
- Zhang JQ, Yan Y (2003). On-line Continuous Measurement of Particle Size Using Electrostatic Sensors. *Powder Technol.* 135-136:164-168.